Identity of the reversible hole traps in InP/ZnSe core/shell quantum dots

Anne Myers Kelley[1]*, Paul Cavanaugh[1a], Haochen Sun[1a], Xudong Wang,[2] Maria J. Bautista,[2] Ilan Jen-La Plante,[2] Christian Ippen,[2] and David F. Kelley[1]*

[1]Department of Chemistry and Biochemistry, University of California Merced, 5200 North Lake Road, Merced, CA 95343

[2]Nanosys Inc., 233 S. Hillview Dr, Milpitas, CA 95035

*Authors to whom correspondence should be addressed: amkelley@ucmerced.edu, dfkelley@ucmerced.edu

[a]These authors contributed equally to this work.

Abstract

Density functional theory calculations are combined with time-resolved photoluminescence experiments to identify the species responsible for reversible trapping of holes following photoexcitation of InP/ZnSe/ZnS core/shell/shell quantum dots (QDs) having excess indium in the shell (Cavanaugh *et al*., J. Chem. Phys. **155**, 244705, 2021). Several possible assignments are considered, and a substitutional indium adjacent to a zinc vacancy, In^{3+}/V_{Zn}^{2-}, is found to be the most likely. This assignment is consistent with the observation that trapping occurs only when the QD has excess indium and is supported by experiments showing that the addition of zinc oleate or acetate decreases the extent of trapping, presumably by filling some of the vacancy traps. We also show that addition of alkyl carboxylic acids causes increased trapping, presumably by creation of additional zinc vacancies. The calculations show that either a single In^{2+} ion or an In^{2+}-In^{3+} dimer is much too easily oxidized to form the reversible traps observed experimentally, while In^{3+} is far too difficult to oxidize. Additional experimental data on InP/ZnSe/ZnS QDs synthesized in the absence of chloride demonstrates that the reversible traps are not associated with Cl^-. However, a zinc vacancy adjacent to a substitutional indium is calculated to have its highest occupied orbitals about 1 eV above the top of the valence band of bulk ZnSe, in the appropriate energy range to act as reversible traps for quantum confined holes in the InP valence band. The associated orbitals are predominantly composed of p orbitals on the Se atoms adjacent to the Zn vacancy.

Introduction

Semiconductors nominally composed of a single material often contain impurities that influence their electronic and optical properties.[1-3] In particular, impurity species may provide energy levels that fall within the band gap of the pure semiconductor and can thereby act as traps for either electrons or holes. If the energy level is sufficiently far below that of the conduction band (for electrons) or above that of the valence band (for holes), then the trapping is essentially irreversible at ambient temperatures; once the electron or hole finds the trap, it never gets out and ultimately undergoes radiative or nonradiative recombination with the other carrier. However, if the energy levels of the trap are close enough to those of the valence or conduction band it is also possible to have reversible trapping, where the trapped and untrapped electron or hole are in equilibrium. While carrier trapping often plays a central role in determining the overall photophysics, it is unusual that the chemical and structural nature of the trap can be assigned.

An interesting case of reversible hole trapping has recently been shown to occur in InP/ZnSe/ZnS core/shell/shell quantum dots (QDs) containing indium impurities in the ZnSe shell.[4-5] InP/ZnSe is a "quasi-type II" structure as shown in Figure 1. Bulk InP has a higher valence band energy and a lower conduction band energy than ZnSe, but when quantum confined in a small QD the lowest energy wavefunction of the electron is delocalized over core and shell, while the lowest energy hole wavefunction is largely confined to the InP core.[6] Excitation at a photon energy well above the band-edge transition creates a mixture of excitonic states distributed throughout the InP core and the much larger-volume ZnSe shell. Following high energy photoexcitation, the band-edge photoluminescence (PL) in most types of QDs, for example CdSe, is observed to rise within the approximately 40 ps time resolution of the time-correlated single photon counting experiments. By analogy, both the electron and the hole in

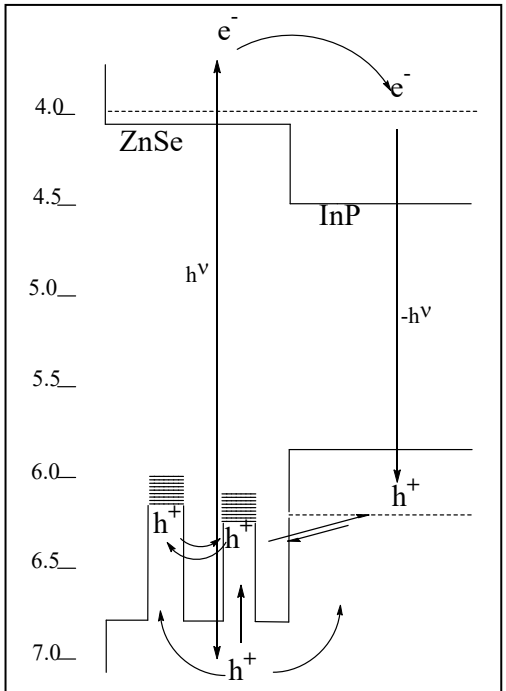

Figure 1. Energy level diagram for InP/ZnSe QDs showing the hole trapping dynamics inferred from time-resolved photoluminescence measurements.

InP/ZnSe/ZnS QDs would be expected to rapidly cool to the band edge. However, in InP/ZnSe/ZnS core/shell/shell QDs with excess indium in the ZnSe shell, some fraction of the PL was found to rise on a time scale of >100 ps.[4-5] In addition, QDs with large slow risetime components also show significant delayed emission.[5] The PL kinetics show a weak and complicated temperature dependence in the 23 – 70 °C range, indicating that the traps are in close energetic proximity to the band edge state. Despite there being no broad and red-shifted emission typically associated with carrier trapping, the apparent radiative lifetime in such structures was significantly longer than in "stoichiometric" structures, those without excess indium.[5] These observations led to the conclusion that the ZnSe shell contains indium-associated hole traps having energies sufficiently close to the valence band edge to allow reversible hole trapping and detrapping. A hole population that is in equilibrium between the valence band and the trap states gives rise to the observed longer radiative lifetime of the band edge state – there is both prompt and delayed band edge emission. Other workers have examined indium doping of the ZnSe shell in InP/ZnSe core/shell QDs and attributed reduced PL quantum yields to the indium impurities.[7-8] Furthermore, green-emitting InP/ZnSe/ZnS QDs having excess indium in the shell have been found to exhibit red-shifted emission from trap states.[9] In the present case, population of the traps occurs while maintaining a very high overall PL quantum yield, typically greater than 90%, and there is no detectable trap emission.

The observed dynamics require that the traps have energies close to that of the quantum confined hole, and consideration of these energetics is crucial to assigning the trapping species. Estimates of the InP-ZnSe valence band offset vary over a significant range, from about 0.5 to 1.0 eV. Perhaps the most reliable estimate is from photoemission data, which puts the valence band offset at 0.97 eV.[10] In the case of red-emitting QDs the hole quantum confinement energy is calculated to be 0.22 eV, putting the quantum confined hole energy 0.75 eV above (closer to the vacuum level) the ZnSe valence band edge. If the trap is in thermal equilibrium with the valence band, then the trap energy is within about kT (26 meV) of this value. The uncertainty of this value is partially determined by the uncertainty of the InP-ZnSe valence band offset. Furthermore, this trap depth is necessarily approximate because the presence of internal electric fields could easily shift the trapped hole versus valence band energies by several tens of milli-electron volts.

Although the data show that these reversible hole traps are associated with excess indium in the shell, the chemical and structural nature of the traps remains unclear. The indium in the core is nominally In^{3+} and further oxidation of this species is unlikely. However, several other possibilities can be considered. Reduction of the indium to In^{2+} prior to its incorporation in the ZnSe shell might provide the possibility of a reversible hole trap based on the In^{2+}/In^{3+} redox couple. This is analogous to Cu^{+} being oxidized to Cu^{2+} and thereby acting as a hole trap in CdSe nanocrystals.[11] The known binary compound of In(II) with Se, InSe, is a layered structure containing In-In bonds, and the possibility of an indium dimer in the shell being the trapping species can be considered. Alternatively, the trap might be localized on another species whose presence is enabled by incorporation of indium into the shell. Many of the InP/ZnSe syntheses involve the use of $ZnCl_2$ and therefore have a high concentration of chloride ions during shell growth. These Cl^- ions might be incorporated into the ZnSe lattice as dopants, perhaps interstitially with the extra negative charge compensated by a $Zn^{2+} \rightarrow In^{3+}$ substitution. Another possible assignment of the trap is to a zinc vacancy partially charge compensated by the presence of an adjacent substitutional In^{3+}. In bulk ZnSe, ODMR results show that zinc vacancies with a -2 charge (V_{Zn}^{2-}) give rise to an energy level 0.66 eV above the top of the ZnSe valence band.[12-13] This measured energy is consistent with values recently obtained from DFT calculations, confirming the assignment.[14] Zinc vacancies in bulk ZnSe that are charge compensated by an adjacent (substitutional) In^{3+} ion have also been studied and their energetics determined by transient photocurrent measurements.[15] These measurements put the acceptor energy of the singly charged vacancy adjacent to the In^{3+} (the In^{3+}/V_{Zn}^{-} electron acceptor or In^{3+}/V_{Zn}^{2-} hole acceptor complex) close to that of the zinc vacancy, 0.59 eV above the ZnSe valence band. Localization of the trapped hole results in a strong local electric field which distorts the surrounding lattice. Thus, the trapping energy includes a significant contribution from electron-phonon coupling, as found for surface traps in CdSe and CdS.[16-18] This energy is 0.16 eV lower than that inferred above for the valence band hole, which is well within the uncertainty of the reported band offsets. It follows from these energetics that the presence of the adjacent In^{3+} stabilizes the doubly negatively charged zinc vacancy and makes it about 70 meV harder to oxidize.

The present work considers several possibilities and identifies the traps as the In^{3+}/V_{Zn}^{2-} species through a combination of experiment and calculation. The experiments involve time-

resolved photoluminescence studies showing that it is possible to increase the trap density by reaction with oleic acid and decrease the trap density by the reaction with zinc oleate or zinc acetate. Density functional theory calculations on small ZnSe clusters containing different indium-associated impurities were used to characterize several possible trapping species. The assignment to the In^{3+}/V_{Zn}^{2-} species is supported by literature precedents and by both experiment and calculation.

Experimental methods

The QDs and experimental methods used in this study are largely the same as in previous reports.[4-5] These are very high quality InP/ZnSe/ZnS QDs having PL linewidths of about 40 nm and quantum yields of typically 90%. Most of the experimental results are on "core-derivatized" QDs in which the InP core is reacted with excess Zn^{2+} and subsequently purified prior to growth of the ZnSe shell. The core-derivatized QDs having a 2.9 nm diameter core and a shell thickness that is calculated from the elemental ratios to be 2.72 nm (referred to as CD-2.72 in a previous publication[5]) show very large and easily quantifiable PL rise kinetics and were extensively used in the present study. These particles have a very thin (submonolayer) ZnS outer shell. The absorption and PL spectra and TEM and HRTEM images of the particles are given in the Supplementary Material. Nonstoichiometric QDs are synthesized with very similar cores and the same shell growth conditions, but without the Zn^{2+} treatment and subsequent purification. In some cases, these particles were dissolved in toluene containing excess zinc oleate, zinc acetate, or oleic acid. In a typical treatment, a combination of 20 μL QD sample solution (containing approximately 1.2 μmol QDs) and 4.0 mL dried toluene were mixed in a 25-mL three-neck flask, then a 0.33 mL solution of 0.61 M zinc oleate in 1-octadecene (0.20 mmol zinc oleate), or 40 μL of oleic acid (0.13 mmol oleic acid), or 92 mg of anhydrous zinc acetate powder (0.50 mmol zinc acetate) was added to the mixture. In some cases, the mixture was heated to 100 ^{o}C under nitrogen for 1 hour and then cooled to room temperature. In the case of zinc acetate, the mixture was vigorously stirred overnight. In all cases, the QD surfaces are primarily zinc oleate terminated and the sample was kept in nitrogen overnight prior to PL kinetics measurements. We also report results on nonstoichiometric particles having slightly smaller cores (2.55 nm diameter) and approximately 2.58 nm thick ZnSe shells. These QDs were synthesized either chloride free or with the shell grown under conditions of excess $ZnCl_2$. The

spectroscopic methods used here are the same as reported in previous publications.[4-5] We note that the time-resolved PL measurements were made by time-correlated single photon-counting. The temporal instrument response of this apparatus is limited by the response of the single-photon avalanche detector. It is characterized by a ≈ 40 ps Gaussian and a wavelength dependent exponential tail, as described in reference 5. The PL kinetics were found to be only very weakly dependent on the detection wavelength. The kinetics presented below were obtained with detection at the PL maximum.

Computational methods

The computational methods employed in this study were adapted from those used by Nelson *et al*. for copper and silver dopants in CdSe QDs.[11, 19] Approximately spherical nanocrystals of ZnSe having 31, 34, 49, or 53 formula units were initially constructed by starting from a zincblende bulk lattice. Surface atoms that did not have four nearest neighbors were made fully coordinated by adding pseudo-hydrogen atoms in a tetrahedral geometry. Pseudo-H atoms have the electronic properties of hydrogen but have a variable nuclear charge and mass. Pseudo-H atoms attached to Zn were given a nuclear charge of 1.5 (thus pulling electron density away from the Zn as a bound Se would) and a mass of 79 (the same mass as Se, for minimal perturbation of the vibrational frequencies). Pseudo-H atoms attached to Se were given a nuclear charge of 0.5 (thus donating electrons as a bound Zn would) and a mass of 65 (that of Zn). Density functional theory calculations were performed using Gaussian 16[20] with the PBE0 hybrid density functional and the Los Alamos double-zeta basis set and pseudocore potential. All results shown are on structures for which the geometry has been optimized. Orbitals were visualized using the natural orbital analysis and are displayed with an isosurface value of 0.02.

Structures incorporating indium were constructed by replacing one of the zinc atoms close to the center of the structure with indium. Zinc vacancies were created by removing one of the zinc atoms close to the center, separated by one Se atom from the indium in substituted structures. The pure ZnSe structures have zero charge (formally, Zn^{2+} and Se^{2-}) and are spin singlets. Structures with substitutional indium were calculated either as charge-neutral doublets (formally, In^{2+} replacing Zn^{2+}) or as positively charged singlets (In^{3+} replacing Zn^{2+}). Structures with both a substitutional indium and a zinc vacancy were calculated as negatively

charged singlets (removing one Zn^{2+} and substituting In^{3+} for another Zn^{2+}). Following Li and Gamelin,[11, 19, 21] a +q or -q charge on the core was compensated by reducing or increasing the nuclear charges on each of the N pseudo-H atoms by q/N.

A few calculations were also carried out using an expanded basis set including d orbitals on Se, and using two different exchange-correlation functionals, HSE06[22] and M06-2x.[23] These results are described in the Supplementary Material.

Quantum confinement energies were calculated using an empirically-corrected effective mass approximation method.[4, 6, 24]

Results and Discussion

The possibility of the trap involving different indium-based defects in the ZnSe shell is assessed through DFT calculation of the hole accepting energy. The starting point is density functional calculations on the four pure ZnSe clusters ($Zn_{31}Se_{31}H_{66}$, $Zn_{34}Se_{34}H_{66}$, $Zn_{49}Se_{49}H_{78}$, and $Zn_{53}Se_{53}H_{86}$). All of these clusters optimize to structures with approximately tetrahedral bonding and all Zn-Se bond lengths between 2.51 and 2.57 Å. The highest occupied molecular orbital (HOMO) is at -7.19, -7.18, -7.10, and -7.07 eV for the clusters with 31, 34, 49, and 53 formula units, respectively, rising slightly in energy with increasing size as expected. The cluster with 53 formula units has a diameter of about 1.6 nm, which, extrapolating slightly from the data of ref. 25, has an experimental lowest excitonic transition energy of about 4.0 eV, 1.3 eV above the bulk band gap. Using electron and hole effective masses of 0.16[26] and 1.44,[27] respectively, the hole confinement energy is estimated to be about 0.13 eV, which would put the calculated top of the bulk ZnSe valence band at -6.94 eV, in good agreement with the experimental value of -6.82 eV.[10] While absolute energies calculated with DFT are not always very accurate, the close agreement between experiment and calculation for the energy of the top of the bulk ZnSe valence band suggests that calculated orbital energies for other structures should also be reliable. As such, throughout this paper we will directly compare trap energies obtained from DFT calculations with the literature valence band energies.

Figure 2 shows the HOMO and HOMO-1 for the largest cluster. The HOMO and the several orbitals immediately below it are composed almost entirely of Se p orbitals and are largely delocalized throughout the cluster, as expected.

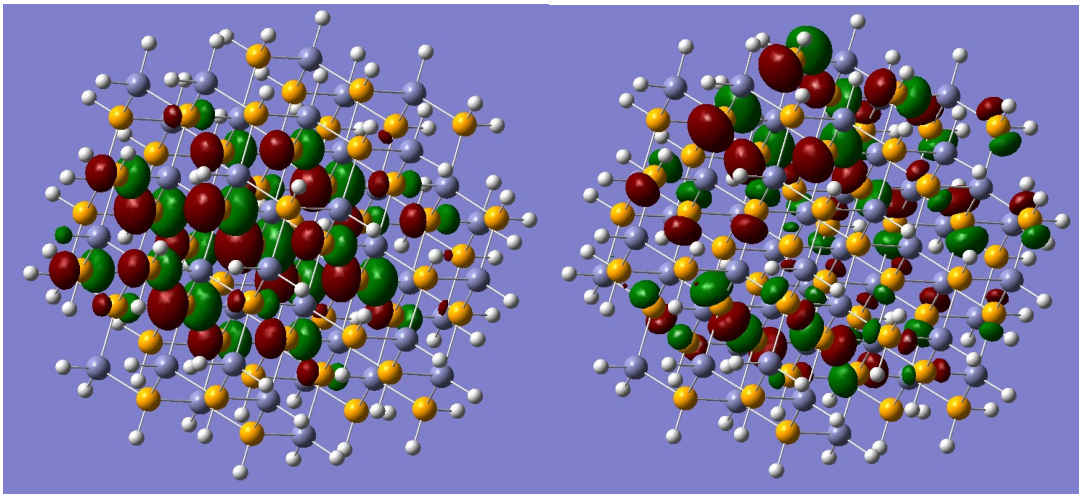

Figure 2. Highest occupied molecular orbital (HOMO), left, and HOMO-1, right, calculated for $Zn_{53}Se_{53}H_{86}$. The structure has C_{3v} symmetry and the HOMO-1 is doubly degenerate; only one of the two degenerate orbitals is shown. Zn, Se, and H atoms are blue, yellow, and white, respectively.

Replacement of one of the central Zn atoms by In ($Zn^{2+} \rightarrow In^{2+}$) in the 34 cluster gives a singly occupied HOMO at -4.30 eV, localized almost entirely on the In atom, and the HOMO-1 at -7.20 eV, a combination of Se p orbitals having nearly the same energy and orbital description as in the pure ZnSe cluster. Clearly a single In^{2+} impurity serves as an excellent hole trap, readily oxidized to In^{3+} by accepting a hole (losing an electron). However, this is a very deep trap and would not be reversible. Incorporation of In^{2+} into the ZnSe crystal also requires considerable distortion of the lattice; the Zn-Se bond lengths at the optimized geometry are 2.51-2.57 Å in the pure ZnSe structure, while the In-Se distances are 2.80-2.84 Å in the In^{2+}-substituted structure. Replacement of one of Zn ions by In^{3+} instead gives a doubly occupied HOMO at -7.26 eV which is almost entirely composed of Se p orbitals, and the In-Se bond lengths are 2.61-2.62 Å, only slightly perturbed relative to the pure ZnSe lattice. Thus, while In^{3+} fits into the ZnSe lattice fairly well, it would not provide energy levels that could serve as hole traps; In^{3+} is not going to be oxidized to In^{4+}.

The possibility that the trap is an In^{2+}-In^{2+} or In^{2+}-In^{3+} dimer was also explored in the structure with 34 formula units by replacing two next-nearest-neighbor zinc ions with indium and slightly deforming the starting structure to bring the two indium atoms closer together. Optimization of the geometry for the In^{2+}-In^{2+} case produced a structure with an In-In distance of 2.86 Å, In-Se bond lengths of 2.75-2.90 Å, and a very badly strained In-Se-In bond angle of 60

degrees. The HOMO and LUMO of this structure are essentially the In-In bonding and antibonding orbitals. The HOMO energy is -5.18 eV, lower than in the single In^{2+} system but still much too high to serve as a reversible trap. In the In^{2+}-In^{3+} case, a single electron in the In-In bonding orbital does not confer enough stability to offset the large lattice distortion required to bring the indium atoms together and the structure reverts to a slightly perturbed ZnSe lattice with an In-In distance of 4.64 Å and an In-Se-In bond angle of 115 degrees. The singly occupied HOMO in this case is composed almost entirely of one indium s orbital and the p orbitals from its four coordinated Se atoms, but the HOMO energy of -5.11 eV is almost the same as for the In^{2+}-In^{2+} case.

These calculations indicate that a reversible hole trap cannot be centered on an indium ion or pair of indiums. Indium is too easy to oxidize in its +2 oxidation state, whether in monomeric or dimeric form, and too hard to oxidize in its +3 oxidation state. Yet the experimental data show that the existence of reversible hole traps depends on the amount and distribution of indium in the shell. Metal chlorides are often used in the synthesis of InP/ZnSe QDs, and another possibility is that the trap involves an interstitial chloride ion, charge compensated by a substitutional In^{3+}. However, QDs that are rigorously chloride free exhibit PL risetime kinetics that are very similar to those previously reported for nonstoichiometric QDs.[4-5] This eliminates the possibility that the trap can be assigned to Cl^- ions charge compensated by In^{3+}.

Assignment to an In^{3+}/V_{Zn}^{2-} species is consistent with several experimental results. Significant trapping requires the presence of at least a small indium excess. Furthermore, in QDs having an overall indium concentration that exceeds a small excess, the extent of trapping is indium concentration independent. This implies that not all In^{3+} dopants are associated with traps and that zinc vacancies, by themselves, either do not occur at significant concentrations or are not hole traps. Two types of experimental results indicate that while in a specific QD ensemble the indium concentration is constant, the vacancy concentration can be varied. These results involve measuring the PL risetime kinetics of the CD-2.72 QDs following reaction with excess zinc carboxylate or excess carboxylic acid. The CD-2.72 QDs are chosen for these studies because prior to any treatment, they exhibit a large, slow risetime component in the PL kinetics that can be easily and accurately measured.[5]

Figure 3 shows that exposure to excess oleic acid or zinc oleate results in significant changes in the fraction of the PL showing a slow risetime. This occurs by shifting the equilibrium of the vacancy formation reaction, eq. (1):

$$2RCOO^- + QD(V_{Zn}^{2-})_n \quad \rightleftharpoons \quad Zn(RCOO)_2 + QD(V_{Zn}^{2-})_{n+1} \qquad (1)$$

Addition of alkyl carboxylic acids or zinc carboxylates shifts the reaction equilibrium toward products or reactants, respectively, as one would expect from Le Chatelier's principle. Figure 3 shows that addition of excess oleic acid at room temperature results in a small, but significant increase in the magnitude of the slow rise component. In this case, the presence of excess oleate pulls out zinc ions, creating more zinc vacancies. Conversely, the addition of excess zinc oleate significantly reduces the magnitude of the slowly rising PL component, indicating that some of the zinc vacancies have been filled. Addition of zinc oleate or oleic acid shifts the eq. (1) equilibrium in opposite directions, but in both cases results in negligible changes (less than a few percent) in the PL quantum yield. Shifting the equilibrium in eq. (1) either way involves diffusion of zinc ions through the ZnSe and ZnS shell lattices of the QD (the ZnS shell is less than one monolayer thick in these samples). This type of reaction is quite plausible; it is known through ion exchange studies on other types of QDs that the metals are quite mobile, even at room temperature.[28-31]

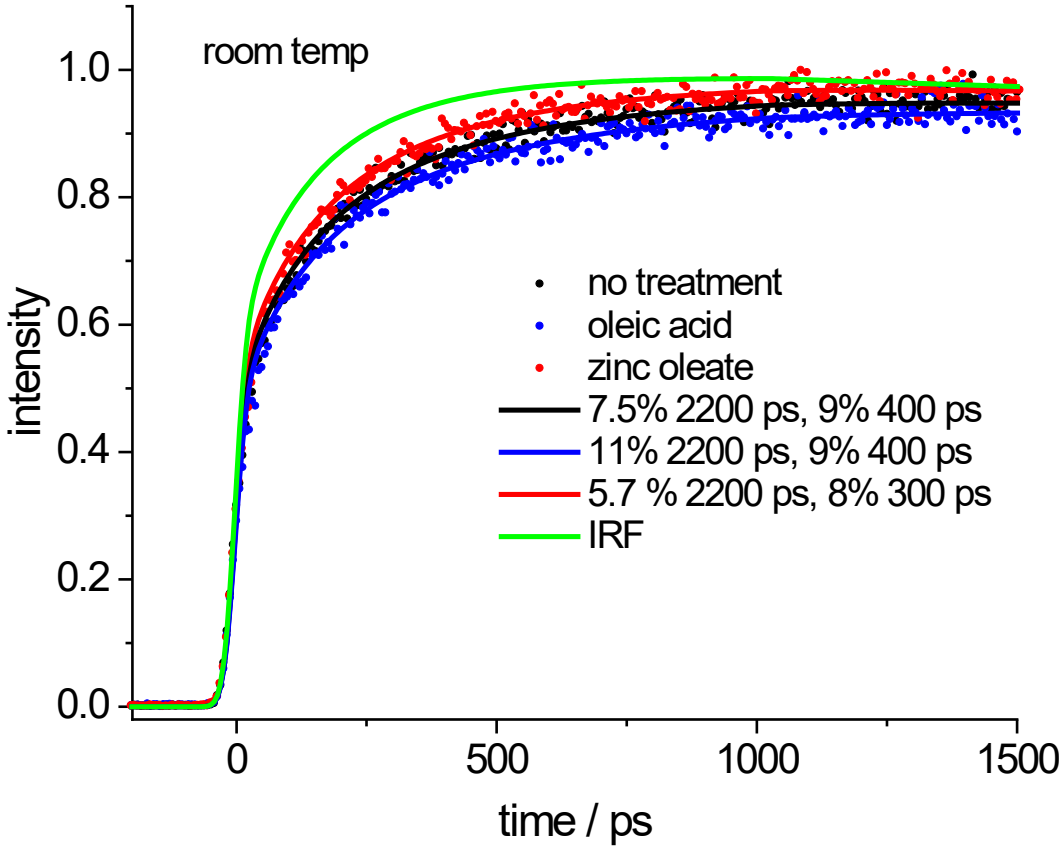

Figure 3. Normalized PL kinetics for QDs following no treatment, room temperature exposure to excess zinc oleate, and room temperature exposure to excess oleic acid. Also shown are calculated curves corresponding to an instantaneous risetime (IRF) and to an instantaneous risetime plus the indicated slower risetimes, each convolved with the temporal instrument response function.

An obvious question is whether eq. (1) is in equilibrium immediately following the addition of zinc oleate or oleic acid, or whether the approach to equilibrium at room temperature is slow. To address this question, we have performed this reaction with zinc acetate at room temperature and zinc oleate at room temperature and 100 °C. We note that the corresponding reaction with zinc acetate cannot be run at 100 °C; the surface ligands become labile at elevated temperatures and the oleate ligands can be replaced by acetate, resulting in the loss of colloidal stability. Figure 4 shows that following treatment at room temperature, the risetimes with zinc oleate and acetate are essentially identical. Figure 4 also shows that the reaction with zinc oleate at 100 °C results in a decrease in the risetime that is larger than that obtained at room temperature. This is especially true for the slowest risetime component. Diffusion of the zinc ions through the ZnSe lattice is expected to be faster at elevated temperatures. The temperature

dependence of the fraction of vacancies that are filled suggests ion diffusion through the lattice, rather than solution diffusion of the zinc precursor species, is the rate limiting step in this reaction. However, the observed temperature dependence may also reflect a temperature dependence of the eq. (1) equilibrium constant, with incomplete relaxation of the higher temperature equilibrium upon cooling.

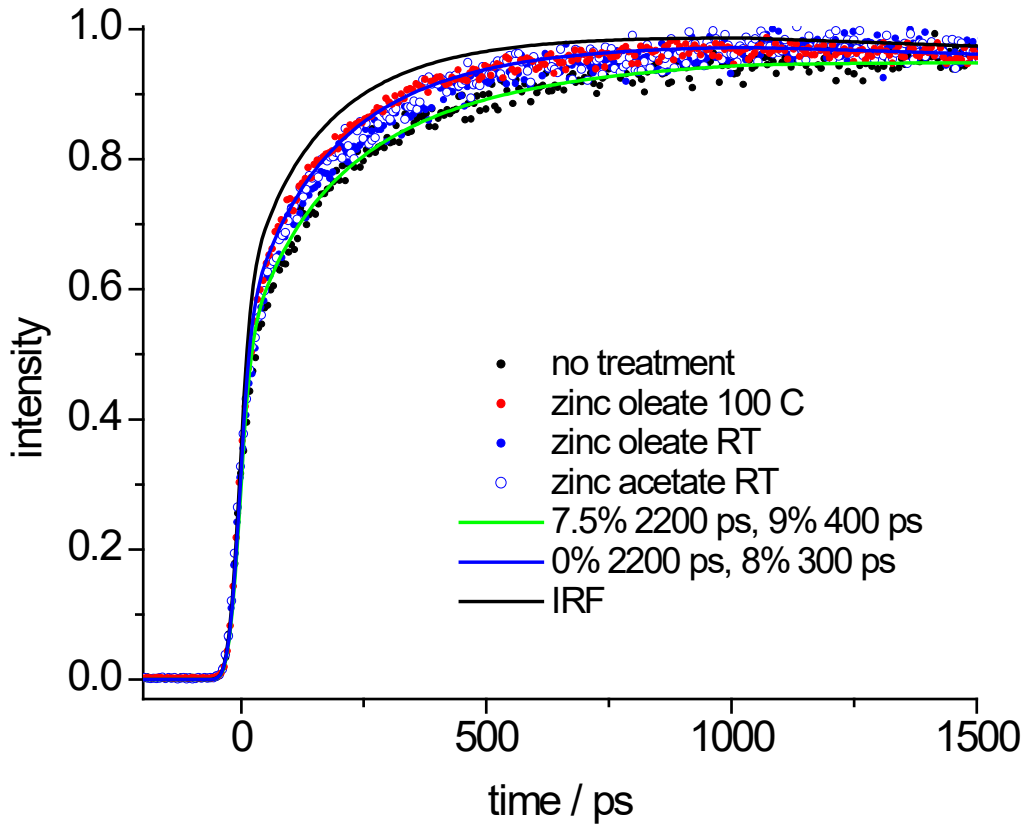

Figure 4. Normalized PL kinetics for QDs following exposure to excess zinc oleate and zinc acetate at room temperature, zinc oleate at 100 °C, and the PL kinetics before treatment. Also shown are calculated curves corresponding to an instantaneous risetime (IRF) and to an instantaneous risetime plus the indicated slower risetimes, each convolved with the temporal instrument response function.

We note that much larger slow risetime components are observed in the core-derivatized QDs compared to nonstoichiometric QDs, indicating that the core-derivatized QDs have much higher trap densities.[5] This observation is also consistent with the assignment of the traps to In^{3+}/V_{Zn}^{2-} impurities. The essential difference between these types of QDs is the nature of the

core-shell interface. The core-derivatized QDs have had the cores treated with an excess of zinc carboxylate, added to the reaction mixture immediately following core growth. This results in zinc ion adsorption and/or indium-to-zinc ion exchange on the core surface. Thus, we conclude that in the core-derivatized QDs, the core-shell interface consists primarily of P-Zn, rather than In-Se bonding, which is consistent with the Raman spectroscopy on these QDs.[5] This has two possible effects on the shell-localized traps. First, the different types of core-shell bonds will result in very different electric fields across the shell and thus different valence band potentials. Specifically, the presence of nominally Zn^{2+} at the core-shell interface will result in a more positive net charge in the interior of the QDs. This will stabilize the net negative charge on the In^{3+}/V_{Zn}^{2-} impurity. Second, the P-Zn bonding partially mitigates the lattice strain associated with the mismatch of InP and ZnSe lattice constants. The lattice mismatch expands the ZnSe lattice, and this effect is minimized in the case of the core-derivatized QDs. The DFT calculations show that the presence of a zinc vacancy locally contracts the lattice (see Supplementary Material). Lattice contraction is energetically less favorable when the lattice has been expanded by the presence of the interface with InP. Thus, we suggest that vacancy formation is more energetically favorable, and this results in the core-derivatized QDs having greater trap densities than their nonstoichiometric counterparts.

The assignment of the traps to In^{3+}/V_{Zn}^{2-} impurities is also consistent with the energetics obtained from the computational results. For each of the four starting clusters (31, 34, 49, and 53 formula units), we carried out calculations on structures having a zinc vacancy and a zinc to indium substitution at neighboring cation sites with an overall charge on the cluster of -1 (*i.e.* remove one Zn^{2+} leaving a V_{Zn}^{2-} vacancy and replace one Zn^{2+} by In^{3+}). As such, these are all closed shell systems having a doubly occupied HOMO. Two different choices for the locations of the indium substitution and the vacancy were examined for each of the three smallest clusters. The HOMOs for these structures ranged in energy from -5.85 to -6.05 eV. The highest occupied molecular orbitals in these structures are composed largely of p orbitals of the Se atoms adjacent to the Zn vacancy. Figure 5 shows the highest occupied orbital for each of the four structures with an indium substitution and zinc vacancy. The energies of the orbitals near the top of the valence band for all of these structures are summarized in Figure 6.

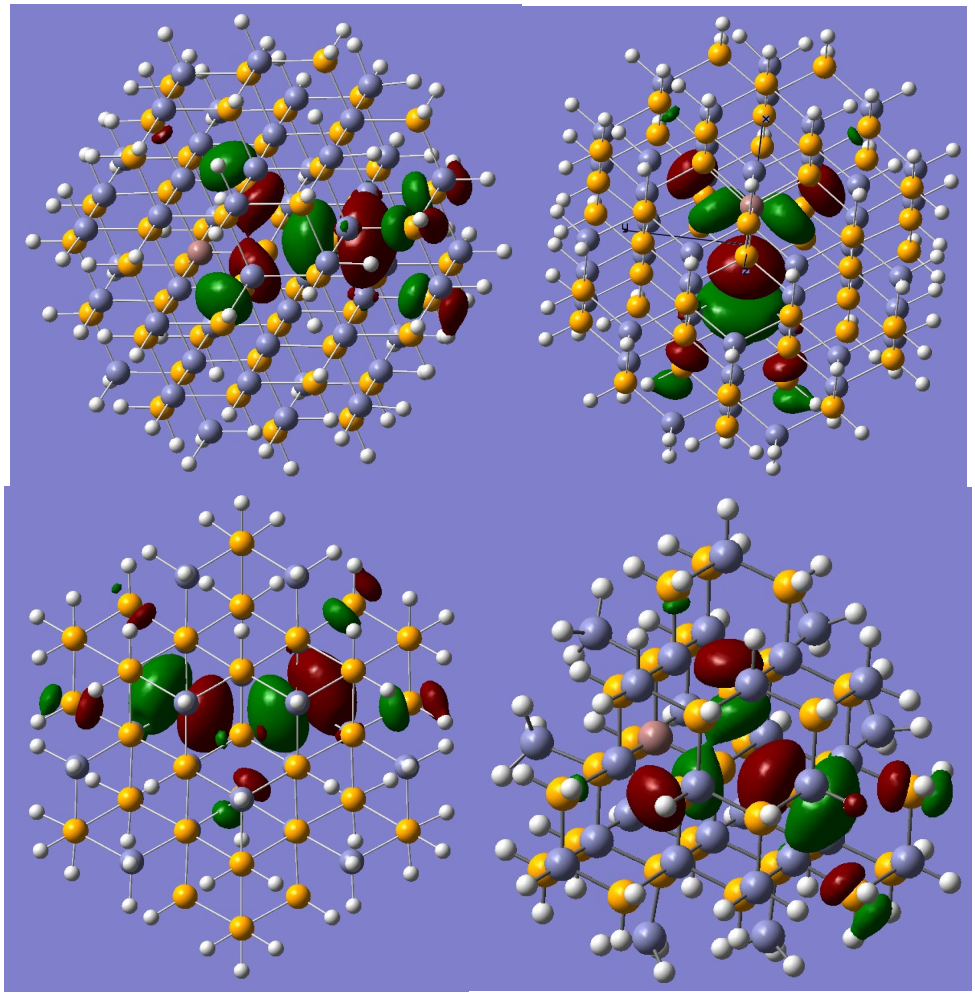

Figure 5. The highest energy occupied orbital of the four ZnSe structures having a zinc vacancy and a substitutional indium (atom in brown). Upper left, upper right, lower left, and lower right show structures with 53, 49, 34, and 31 formula units, respectively, and HOMO energies of -5.89, -5.85, -5.92, and -5.91 eV, respectively.

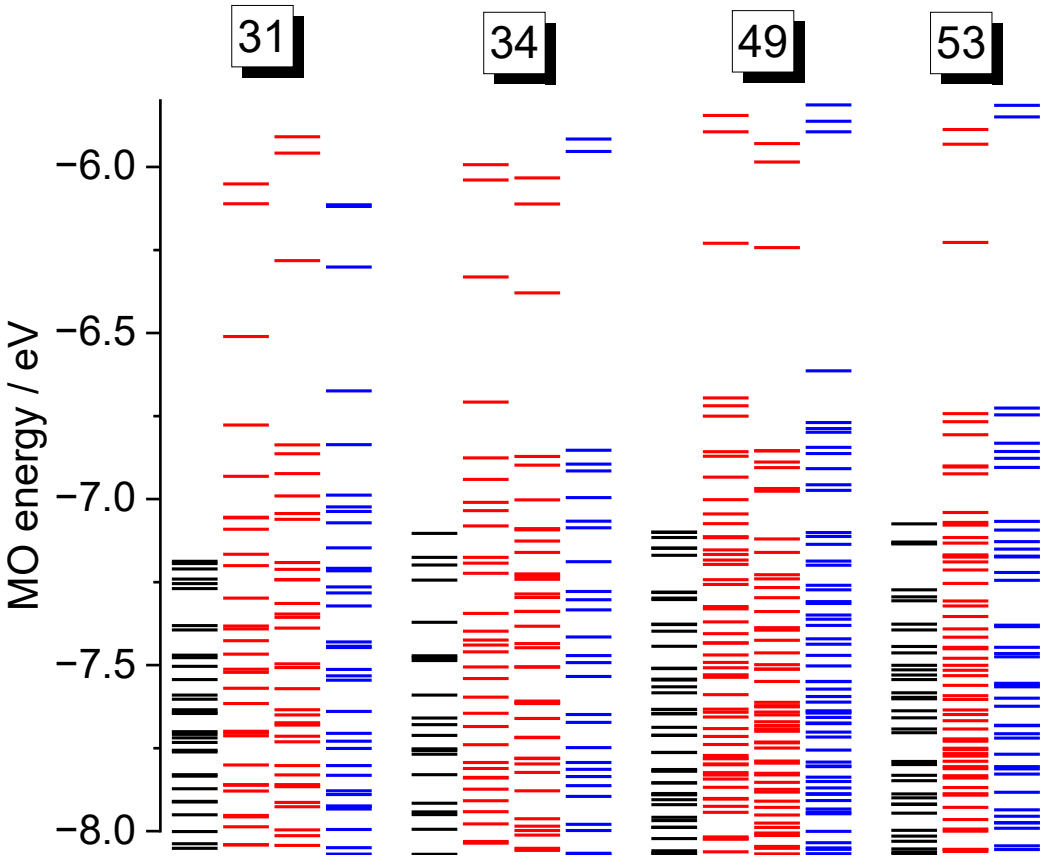

Figure 6. Calculated molecular orbital energies for ZnSe clusters of the indicated sizes with no substitution (black), In^{3+} substitution plus zinc vacancy (red, two different positions for each of the three smallest clusters), and uncompensated zinc vacancy (blue). All calculated orbitals with energies between -8.0 and -2.5 eV are shown, and all of these are doubly occupied.

Calculations were also carried out on clusters having a zinc vacancy without the substitutional indium. In the three largest clusters (34, 49 and 53) these isolated zinc vacancies produced highest occupied molecular orbitals slightly higher in energy (30 to 130 meV) than those of the corresponding indium-compensated vacancies. This is consistent with the experimental data on bulk ZnSe, indicating that an indium-compensated zinc vacancy is about 70 meV more stable and harder to oxidize than an uncompensated vacancy.

The structures on which our DFT calculations are performed are roughly spherical, pure ZnSe clusters with diameters of about 1.2-1.6 nm. The ZnSe shells in the experimental QDs are effectively infinite in two dimensions, and in the other dimension they are 2.6-2.7 nm thick and have interfaces with InP on one side and ZnS on the other. Nevertheless, as the states associated with a zinc vacancy should be spatially localized to the region of the vacancy, our

small systems should be a reasonable though inexact model for vacancies in the experimental systems that are not at the interfaces. As summarized in Figure 6, the calculated In^{3+}/V_{Zn}^{2-} complexes have highest occupied orbitals with energies between -5.85 and -6.05 eV relative to vacuum. Thus, using the experimental ZnSe valence band energy of -6.82 eV, we conclude that the energetics obtained from the calculations reported here give trap depths of 0.77 to 0.97 eV, which are reasonably close to the experimental value of 0.59 eV reported in ref. 15. We note that the calculated trap energies depend on the cluster size and geometry, which suggests that there should be significant inhomogeneity in the trap energies, particularly for those traps located near the interfaces.

The above calculations address the question of the hole energy needed to oxidize the In^{3+}/V_{Zn}^{2-} defect. They do not directly address the energetics of forming these defects. However, the thermodynamics of forming a number of isolated defects and defect complexes in bulk ZnSe have been recently calculated in ref. 14. The results indicate that the zinc vacancy is the most prevalent defect over a significant range of Fermi levels. That work did not address the In^{3+}/V_{Zn}^{2-} complex, but the small lattice distortion associated with the partially charge compensating $Zn^{2+} \rightarrow In^{3+}$ substitution suggests that this defect complex should be even more energetically accessible. Although single-particle HOMO energies may be rather crude approximations to the true trap energies, they should be adequate to rule out the indium-only possibilities for the traps. Furthermore, the calculations together with the experimental data provide strong support for the assignment made.

Apart from its energy, the other characteristic of the hole trap is that radiative recombination with the conduction band electron is nearly or completely forbidden. The calculated HOMOs for the compensated vacancies are composed mainly of p orbitals on the four Se atoms surrounding the vacancy, with only slight participation from other atoms. This hole orbital should have a negligible overlap integral with the electron in the lowest conduction band orbital, which is delocalized over both the InP core and the full ZnSe shell, leading to a negligible rate of radiative recombination.

Conclusions

We have considered a number of possibilities for the chemical/structural identity of the reversible traps observed in the PL dynamics of InP/ZnSe/ZnS QDs. Through a combination

of experiment and calculation, we have arrived at a zinc vacancy (V_{Zn}^{2-}) partially charge compensated by a substitutional In^{3+} as the most likely candidate. This assignment is supported by the closeness of the experimentally inferred trap energies to the energy of the defect level assigned to a zinc vacancy/substitutional indium complex in indium-doped bulk ZnSe,[15] the experiments reported here showing that traps can be added or removed by exposing the QDs to zinc carboxylate or carboxylic acid, and DFT calculations showing that zinc vacancies produce states with appropriate energies and orbital descriptions to serve as traps.

Supplementary Material

Absorption and luminescence spectra; TEM and HRTEM images; calculated energies and molecular orbitals of different cluster sizes, geometries, and substitutions; calculated Se-Se distance distributions for stoichiometric and substituted structures; calculations performed using different density functionals and with an expanded basis.

Acknowledgements

This material is based upon work supported by the U.S. Department of Energy's Office of Energy Efficiency and Renewable Energy (EERE) under the Award Number DE-EE0009164 and NSF grant CHE-1506803. Computing time was provided by the Multi-Environment Computer for Exploration and Discovery (MERCED) cluster at UC Merced, which was funded by NSF grant ACI-1429783. The views expressed herein do not necessarily represent the views of the U.S. Department of Energy or the United States Government. AMK acknowledges helpful discussions with Prof. Xiaosong Li and Prof. Hrant Hratchian.

ORCID

David F. Kelley: 0000-0002-4076-7965

Haochen Sun: 0000-0001-7390-843X

Anne Myers Kelley: 0000-0002-4073-109X

Conflict of Interest

The authors have no conflicts of interest to disclose.

Author Contributions

Anne Myers Kelley: Conceptualization (equal), formal analysis (equal), investigation (equal), methodology (equal), software, visualization, writing/original draft preparation (equal), writing/review and editing (equal). **Paul Cavanaugh**: investigation (equal). **Haochen Sun**: investigation (equal). **Xudong Wang**: investigation (equal). **Maria J. Bautista**: investigation (equal). **Ilan Jen-La Plante**: funding acquisition (equal), investigation (equal), supervision (equal). **Christian Ippen**: investigation (equal). **David F. Kelley**: Conceptualization (equal), formal analysis (equal), funding acquisition (equal), investigation (equal), methodology (equal), supervision (equal), writing/original draft preparation (equal), writing/review and editing (equal).

Data Availability

The data that support the findings of this study are available within the article and its Supplementary Material.

References

1. R. Buonsanti, D. J. Milliron, Chem. Mater. **25**, 1305 (2013).
2. N. Pradhan, S. Das Adhikari, A. Nag, D. D. Sarma, Angew. Chem. Eng. Ed. **56**, 7038 (2017).
3. V. A. Vlaskin, N. Janssen, J. van Rijssel, R. Beaulac, D. R. Gamelin, Nano Lett. **10**, 3670 (2010).
4. A. Nguyen, I. Jen-La Plante, C. Ippen, R. Ma, D. F. Kelley, J. Phys. Chem. C **125**, 4110 (2021).
5. P. Cavanaugh, H. Sun, I. Jen-La Plante, M. J. Bautista, C. Ippen, R. Ma, A. M. Kelley, D. F. Kelley, J. Chem. Phys. **155**, 244705 (2021).
6. H. Lange, D. F. Kelley, J. Phys. Chem. C **124**, 22839 (2020).
7. Y. Li, X. Hou, X. Dai, Z. Yao, L. Lv, Y. Jin, X. Peng, J. Am. Chem. Soc. **141**, 6448 (2019).
8. N. J. Freymeyer, S. M. Click, K. R. Reid, M. F. Chisholm, C. E. Bradsher, J. R. McBride, S. J. Rosenthal, J. Chem. Phys. **152**, 161104 (2020).
9. Y. M. Sung, et al., Small **17**, 2102792 (2021).

10. V. Stevanovic, S. Lany, D. S. Ginley, W. Tumasb, A. Zunger, Phys. Chem. Chem. Phys. **16**, 3706 (2014).

11. H. D. Nelson, X. Li, D. R. Gamelin, J. Phys. Chem. C **120**, 5714−5723 (2016).

12. F. C. Rong, W. A. Barry, J. F. Donegan, G. D. Watkins, Phys. Rev. B **54**, 7779 (1996).

13. D. Y. Jeon, H. P. Gislason, G. D. Watkins, Phys. Rev. B **48**, 7872 (1993).

14. Y. Wu, K. J. Mirrielees, D. L. Irving, Appl. Phys Lett. **120**, 232102 (2022).

15. A. A. Qidwai, J. Woods, J. Cryst. Growth **59**, 217 (1982).

16. M. M. Krause, J. Mooney, P. Kambhampati, ACS Nano **7**, 5922 (2013).

17. T. G. Mack, L. Jethi, P. Kambhampati, J. Phys. Chem. C **121**, 28537 (2017).

18. J. Mooney, M. M. Krause, P. Kambhampati, J. Phys. Chem. C **118**, 7730−7739 (2014).

19. H. D. Nelson, S. O. M. Hinterding, R. Fainblat, S. E. Creutz, X. Li, D. R. Gamelin, J. Am. Chem. Soc. **139**, 6411−6421 (2017).

20. M. J. Frisch, et al. *Gaussian 16, Revision C.01*, Gaussian Inc.: Wallingford, CT, 2016.

21. J. J. Goings, A. M. Schimpf, J. W. May, R. W. Johns, D. R. Gamelin, X. Li, J. Phys. Chem. C **118**, 26584−26590 (2014).

22. A. S. Fuhr, P. Sautet, A. N. Alexandrova, J. Phys. Chem. C **123**, 5705 (2019).

23. P. T. Snee, J. Phys. Chem. C **125**, 11765 (2021).

24. X. Cai, H. Mirafzal, K. Nguyen, V. Leppert, D. F. Kelley, J. Phys. Chem. C **116**, 8118 (2012).

25. V. V. Nikesh, A. D. Lad, S. Kimura, S. Nozaki, S. Mahamuni, J. Appl. Phys. **100**, 113520 (2006).

26. J. L. Merz, H. Kukimoto, K. Nassau, J. W. Shiever, Phys. Rev. B **6**, 545 (1972).

27. C. S. Wang, B. M. Klein, Phys. Rev. B **24**, 3393 (1981).

28. A. R. Freyer, P. C. Sercel, Z. Hou, B. H. Savitzky, L. F. Kourkoutis, A. L. Efros, T. D. Krauss, Nano Lett. **19**, 4797 (2019).

29. A. Sahu, M. S. Kang, A. Kompch, C. Notthoff, A. W. Wills, D. Deng, M. Winterer, C. D. Frisbie, D. J. Norris, Nano Lett. **12**, 2587 (2012).

30. D. H. Son, S. M. Hughes, Y. D. Yin, A. P. Alivisatos, Science **306**, 1009 (2004).

31. R. D. Robinson, B. Sadtler, D. O. Demchenko, C. K. Erdonmez, L.-W. Wang, A. P. Alivisatos, Science **317**, 355 (2007).